

High-speed IR thermography of submerged turbulent water jets

by I. Znamenskaya, E. Koroteeva, A. Novinskaya and N. Sysoev

Lomonosov Moscow State University, Leninskie Gory, 1, 119991 Moscow, Russia, *koroteeva@physics.msu.ru*

Abstract

This work explores the potential of high-speed infrared (IR) thermography to analyze a turbulent water boundary layer in submerged jet flows. In the experiments, the IR camera (FLIR Systems SC7700) is focused on the inner side of an IR-transparent vessel window, providing high-speed (100 Hz) recordings of heat fluxes from a thin water layer close to the window. The temperature variations are shown to act as a passive tracer in the considered turbulent flows. The power spectra of the turbulent fluctuations are calculated for different points in the near-surface flows and compared to the existing theoretical turbulence models.

1. Introduction

High-speed Infrared (IR) thermography is an optical tool capable of visualizing the dynamics of thermal radiation fields and receiving spatio-temporal and spectral characteristics. According to numerous studies performed in the last few years, the IR thermography can be advantageous for analyzing complex thermal flows, due to its high sensitivity and low response time [1, 2]. The recent improvement of the IR cameras in terms of their temporal and spatial resolutions made it possible to acquire the thermal patterns from the surface with the rate up to hundreds of frames per second. This allowed for capturing fast changes in the thermal behavior of flows and, hence, for quantitative studies of unsteady thermal processes including flow turbulence [3, 4].

The IR thermography has been intensively used lately for deeper understanding of the structure of jet flows [5]. In [4] this technique was reported to explore the turbulent heat transfer to air by recording temperature fluctuations on a heated thin-foil. The IR-thermography was applied to study transient and steady impingement of water [6] and air [7] jets; the heat transfer coefficients were calculated by averaging the IR-data. In [8] the IR-thermography and the tomographic PIV were used together for investigation of impinging chevron jets (in comparison with circular jets) in air at Reynolds number 5,000.

Phenomena like an interaction of an impact jet with a wall or mixing of hot and cold jet flows are usually accompanied by flow turbulization. Turbulent flows are complex, unsteady, and characterized by a wide range of length and time scales. The distribution of the kinetic energy over the hierarchy of scales is the key parameter of any turbulent flow. For isotropic turbulence, it is usually evaluated by means of the energy spectrum [9-11]. In the Kolmogorov's model, the process of turbulent mixing consists of energy transmission by the turbulent vortex cascade: the energy of the bigger vortices is transferred to the smaller ones; the smallest vortices dissipate energy into heat. According to the Kolmogorov - Obukhov's law, the spectral density of turbulent energy decreases with increasing of wavenumber under the law of 'five thirds'.

Turbulence is, generally, a three dimensional (3D) phenomenon; with the transition to the two dimensional (2D) flow, a qualitative change of properties and the corresponding pulsation spectra occurs. As theoretically demonstrated, two inertial intervals may coexist in 2D flows: a direct enstrophy cascade to larger scales with a k^{-3} spectrum, and an inverse energy cascade to smaller scales with a $k^{-5/3}$ spectrum [12]. The features of the 2D turbulence are common for large-scale geophysical and astrophysical flows (in this cases it is usually called quasi-two-dimensional turbulence [11, 13]).

Recently, a new technique based on high-speed thermographic measurement has been proposed to study non-isothermal pulsations of turbulent water boundary layers [2, 14, 15]. Since a thin layer of liquid water absorbs almost all the IR-radiation, the time-evolving temperature maps of near-wall boundary layers can be recorded using IR-transparent vessel walls. In the present work, we consider two basic flow configurations of turbulent water mixing process. In experiments, a high-speed IR camera (FLIR Systems SC7700), operating in the spectral range from 3.7 to 4.8 μm , detects time-varying temperature fields in the near-wall boundary layer. We obtain the energy spectra of turbulent near-wall water fluctuations by applying the Fast Fourier Transform (FFT) algorithm to the time dependences of measured thermal signals at selected points of the flow. The results are then compared to the known turbulence models.

2. Experimental setup and procedure

The developed method is based on the differences in the way materials absorb the electromagnetic radiation. Whereas water is almost opaque in the IR camera operating range (3.7 - 4.8 μm), some plastics are highly transparent

in this spectral band [2]. The property of water to absorb infrared radiation at sub-millimeter scale (Fig. 1) allows us to propose a technique of measuring and analysing non-isothermal turbulent fluctuations of fluid flows in the boundary layer through an IR-transparent wall.

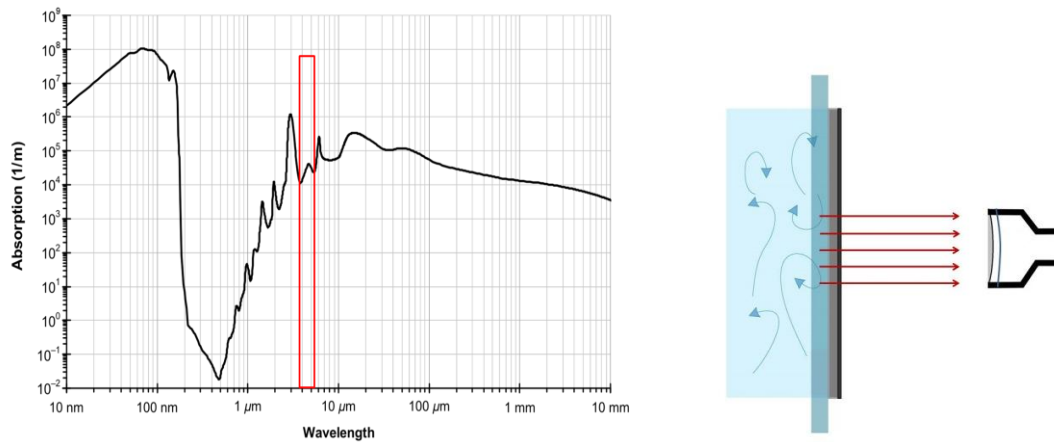


Fig. 1. Absorption spectrum of liquid water adopted from [16], the red square marks the IR camera spectral range (left) and Sketch of the experimental method (right).

In this paper, we consider two basic flow configurations (Fig. 2, left). The first one is a hot impinging jet, submerged in a polypropylene vessel filled with cold water. A thermocouple and a thermometer control the water temperature. The nozzle diameter is $D = 1$ mm. The distance between the nozzle and the impingement surface is set to $h/D \sim 2-4$. Submerged jet directed at a right angle to the surface generates non-isothermal pulsations in the turbulent water boundary layer. The jet flow rate varies, with the maximal flow velocity reaching 22 m/s, which corresponds to the flow Reynolds number $Re \sim 10^6$.

The second configuration consists of a round vessel with two interacting jets (Fig. 2, right). Cold (10-20°C) and hot (30-65°C) water flows enter the vessel through two lateral nozzles of 7 mm diameter. The nozzles intersect at an angle of 120°. A 14-mm-diameter outlet is located at the top of the vessel. The inner diameter and the width of the vessel are 67 and 13 mm, respectively. The average flow velocity from each nozzle is 1.3 m/s ($Re \sim 10^4$).

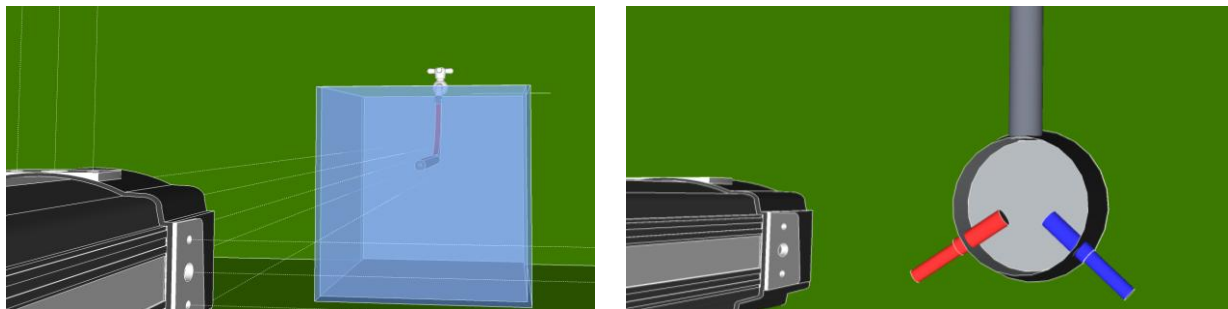


Fig. 2. Scheme of the two experimental arrangements: impinging submerged jet (left) and non-isothermal mixing of two jets (right).

The processes of turbulent water mixing are recorded using an IR camera (FLIR SC7700), having a spectral range of 3.7-4.8 μm and a full-frame resolution of 640 x 512 px. The camera is focused on the inner side of an IR-transparent vessel window, providing high-speed (up to 415 Hz) recordings of heat fluxes emitted from a thin water boundary layer. A standard 50 mm lens and a close-up (macro) lens with 15 μs spatial resolution are used.

In the present experiment, we obtain 1-20 min dynamic thermal recordings. The recording frequency is set to 100-115 Hz. According to the Nyquist theorem, that allows capturing variations of the thermal signal at frequencies up to 50 Hz. Depending on the flow geometry, we select a set of reference points on the obtained thermal movies. The time dependences of measured thermal signals at each point are then processed using the FFT algorithm to calculate the energy power spectra. After that, we determine the characteristic frequencies of temperature pulsations and compute the power laws (f^α) using polynomial interpolation by the method of least squares.

3. Impinging submerged jet

Fig. 3 shows an example of time-varying thermal signals recorded at three selected points on the surface impinged by an axisymmetric hot jet. The most heated is the central region, which is a flow stagnation area ($x/D < 1$). The average water boundary layer temperature decreases to the flow periphery, where the thermal variations, on the other hand, become more pronounced.

The power spectra of turbulent pulsations in the water boundary layer are also calculated (Fig. 3, right). The spectra clearly follow the usual power law $f^{-\alpha}$, where the spectral index is close to the Kolmogorov value (this spectrum is indicated by a red line). This inertial-range scaling of the turbulent energy spectrum is generally observed in three-dimensional fully developed isotropic turbulence [9, 11].

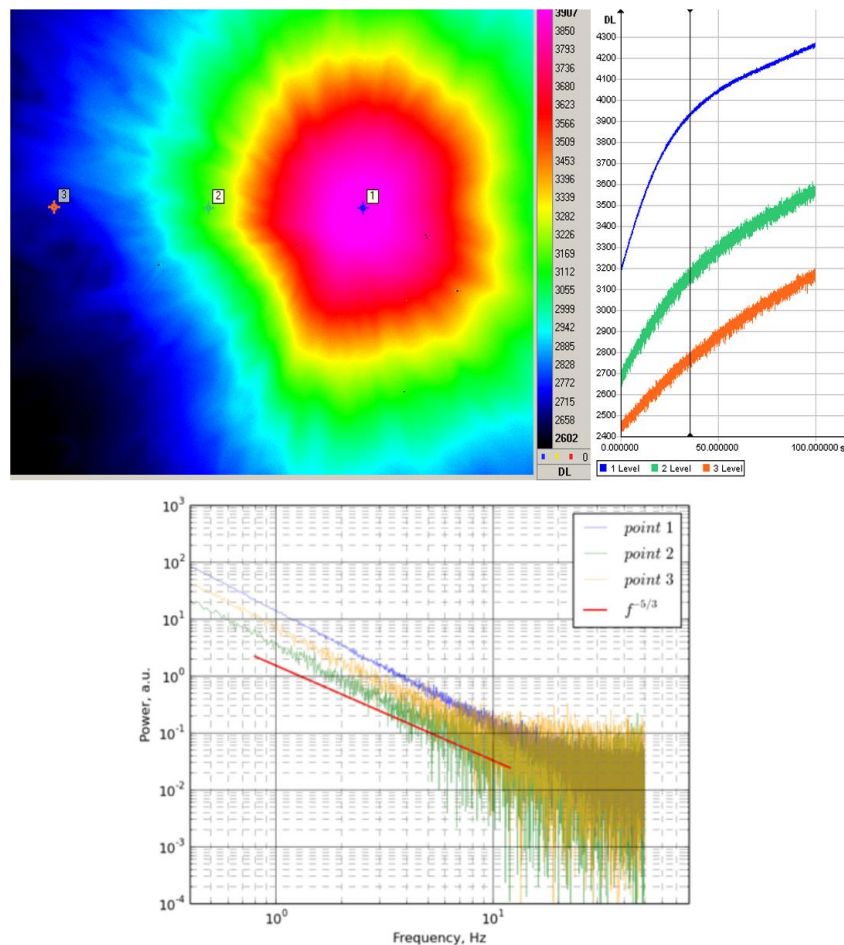


Fig. 3. Typical infrared image of a submerged jet impinging on an IR-transparent wall, obtained using a microscope, with time-varying thermal recordings at 3 selected points (top) and their power spectra (bottom).

We analyze the change in the slope coefficients for the power spectra of water pulsations for different points on the surface. The calculated value of the slope coefficient for the points close to the flow stagnation zone is $\alpha = 2.00 \pm 0.02$. Further from the center, the absolute value of the slope coefficient, α , decreases. In the frequency range of 1-9 Hz, this coefficient is $\alpha = 1.80 \pm 0.05$ at a distance from the nozzle of $x/D = 3$ and $\alpha = 1.70 \pm 0.10$ at $x/D = 6$.

We analyze the dependence of impinging jet spectral characteristics on the jet temperature differences and the jet flow rate. For this purpose, we calculate the power spectra at a point $x/D = 6$ for varying jet impingement conditions:

- the temperature difference between the hot water jet and cold water in the vessel ($\Delta T = 20 - 40^\circ\text{C}$); the jet flow rate remains fixed.
- the jet flow rate (from 5 to 22 m/s); ΔT remains fixed.

Fig. 4 shows that the spectrum corresponding to a greater temperature difference moves slightly higher in the y-axis, since the thermal fluctuations have higher amplitudes. There is no significant difference, however, in the slope coefficient. Fig. 4 also shows no significant change in the energy spectrum for different jet flow rates. These results

confirm our assumption that the temperature can be treated here as a passive contaminant (such as ink). The temperature variations do not govern the fluid motion and, thus, have a tracer function in the flow [17].

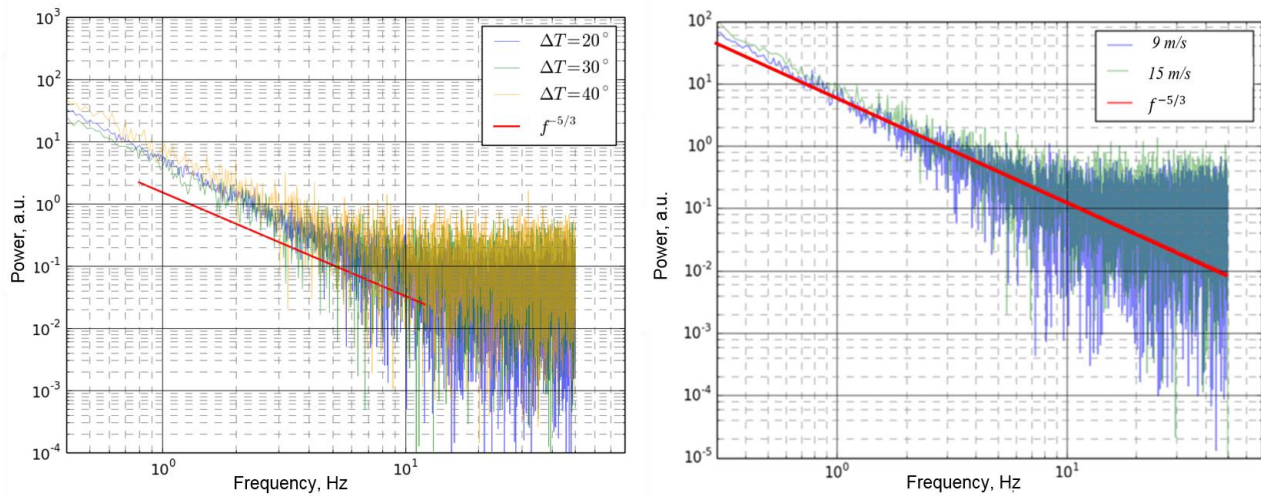


Fig. 4. Power spectra of thermal pulsations: for the fixed flow rate at $\Delta T = 20^\circ\text{C}$ and $\Delta T = 40^\circ\text{C}$ (left); for jet velocity of 9 and 15 m/s at $\Delta T = 40^\circ\text{C}$ (right). Red lines indicate the standard Kolmogorov power spectrum [9].

4. Non-isothermal mixing of two jets

The second set of experiments is conducted to visualize the interaction of two non-isothermal jets in the round disc-shaped vessel. When the jets have the same flow rate, the obtained thermograms have a vertical symmetry (Fig. 5). We consider two fluid flow directions: the vertical axis and the lateral directions along the vessel border.

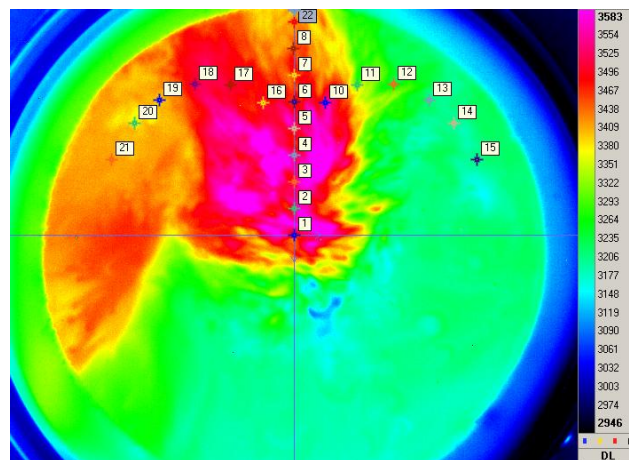


Fig. 5. Typical thermal image of two intersecting jets in the round vessel; jets flow rate is 1.2 m/s, the recording duration is 600 s. Cold and hot water temperatures are 12°C and 52°C .

The spectral analysis of the fluctuations in thermal radiation emitted from the water boundary layer shows:

- 1) For points, located near the symmetry axis, the spectra exhibit two inertial intervals in the ranges of 1-9 Hz and 9-25 Hz (Fig. 6, left).
- 2) For points further from the symmetry axis, the spectral break disappears. The power spectra start following the usual power law $f^{-\alpha}$ (Fig. 6, right).

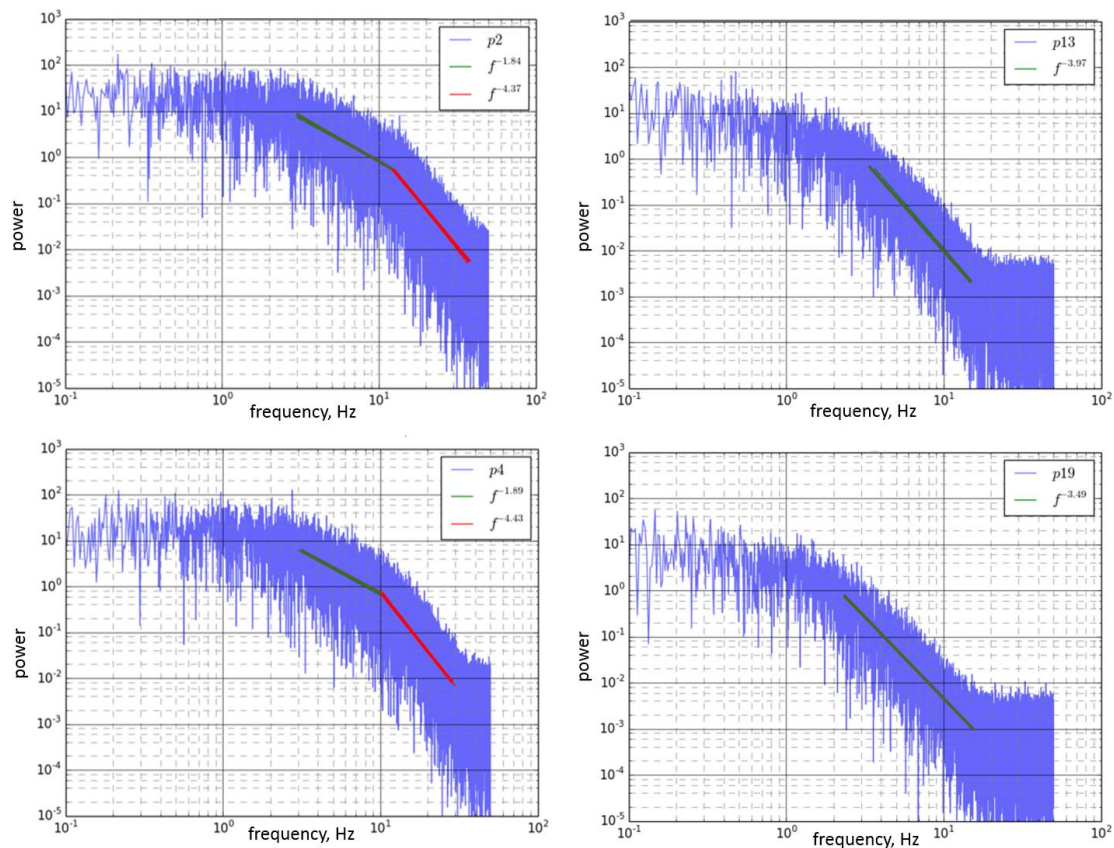


Fig. 6. Power spectra of thermal pulsations at 4 selected points on the thermal image of two intersecting jets in the round vessel; jets flow rate is 1.2 m/s, the recording duration is 300 s. Hot and cold jet temperatures are 48°C and 11°C. Left: points at the central axis; right: peripheral points.

Fig. 6 shows the examples of power spectra for 4 selected points (two central and two peripheral points). Green and red lines, with the given values of calculated slope coefficients, indicate the spectral slopes. On average, for the central points, the slope coefficients are found to be in the range $\alpha = 1.5-1.8$ (frequency interval from 1 to 9 Hz), and $\alpha = 2.9-3.5$ (frequencies interval 9 to 25 Hz). Thus, the first spectral interval is close to the "- 5/3 law", which corresponds to the inverse energy cascade. The second inertial interval, then, can be associated with the direct enstrophy cascade. The formation of the double cascade turbulent spectrum at the central axis may be caused here by the stratification in the near-wall flow, or the flow vorticity.

At a certain high frequency, the spectral amplitude becomes insensitive to frequency changes, and the spectrum enters a horizontal "plateau". This "plateau" frequency depends on the geometric position of the point on the thermogram and decreases away from the vessel center (Fig. 7).

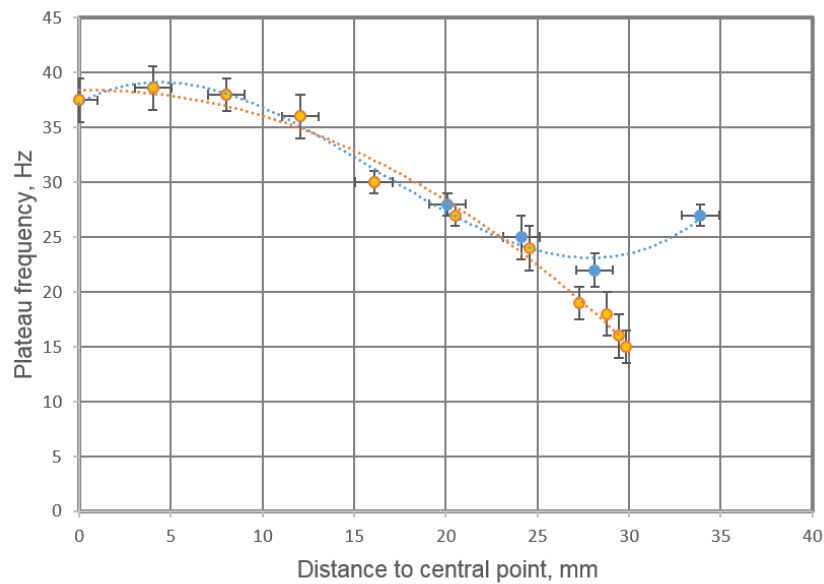


Fig. 7. The dependence of the plateau frequency on the distance from the vessel center. Blue markers - points at the axis, red markers – points at the periphery. Recording duration - 300 s, jets flow rate - 1.2 m/s, hot and jet temperature - 48°C and 11°C.

4. Conclusions

In this work, we have used the high-speed IR thermography to visualize the dynamics of the thermal radiation fields of two basic configurations of a submerged jet flow: a submerged impinging jet and non-isothermal mixing of two jets in a disc-shaped vessel. The IR camera has recorded the radiation emitted from the thin water boundary layer of the considered turbulent flows.

The power spectra of the fluctuating thermal signals have been calculated and analyzed. The results obtained under different experimental conditions (initial temperature differences $\Delta T = 20^{\circ}\text{--}40^{\circ}\text{C}$; jets flow rate 7-22 m/s) have shown that the temperature acts as a passive tracer in the turbulent mixing processes.

The power spectra calculated for different points in the flow have been compared to the spectral behavior predicted by the theory of 2D and 3D turbulent flows. The turbulent fluctuations in the submerged impinging jet follow a power law with a slope close to the Kolmogorov's “-5/3 spectrum” for isotropic 3D turbulence. The thermal pulsations recorded during the mixing of two intersecting jets, on the other hand, has shown the spectral behaviour typical for quasi-2D turbulence. The suggested method, therefore, is fruitful for the quantitative analysis of turbulent boundary layers.

The work is partially supported by RFBR (research project No. 16-38-60186_mol_a_dk) and M.V.Lomonosov Moscow State University Program of Development.

REFERENCES

- [1] Carlomagno G.M., Cardone G., “Infrared thermography for convective heat transfer measurements”. *Experiments in Fluids*, vol. 49(6), pp. 1187–1218, 2010.
- [2] Vavilov V.P., “Infrared thermography and heat control”. *Spectr*, pp. 544, 2013.
- [3] Znamenskaya I.A., Koroteeva E.Y., “Time-resolved thermography of impinging water jet”. *Journal of Flow Visualization and Image Processing*, vol. 20 (1-2), pp. 25–33, 2013.
- [4] Nakamura, H., “Spatio-Temporal Measurement of Convective Heat Transfer Using Infrared Thermography” in *Heat Transfer. Theoretical Analysis Experimental Investigations and Industrial Systems*. Prof. Aziz Belmiloudi (Ed.), InTech, 2011.
- [5] Carlomagno G.M., Ianiro A., “Thermo-fluid-dynamics of submerged jets impinging at short nozzle-to-plate distance”. A review. *Experimental Thermal and Fluid Science*, vol. 58, pp. 15–35, 2014.
- [6] Haustein, H.D., Tebrugge, G., Rohlf, W., Kneer, R., “Local heat transfer coefficient measurement through a visibly-transparent heater under jet-impingement cooling”. *Int. J. Heat Mass Transfer*, vol. 55, pp. 6410–6424, 2012.

- [7] Violato, D., Ianiro, A., Cardone, G., Scarano, F., "Three-dimensional vortex dynamics and convective heat transfer in circular and chevron impinging jets". *Int. J. Heat Fluid Flow*, vol. 37, pp. 22–36, 2012.
- [8] Buchlin J.M., "Convective Heat Transfer in Impinging-Gas-Jet Arrangements". *Journal of Applied Fluid Mechanics*, vol. 4, No. 2, Issue 1, pp. 137 – 149, 2011.
- [9] Kolmogorov A.N., "The local structure of turbulence in incompressible viscous fluid for very large Reynolds numbers", *Proceedings of the Royal Society A*, vol. 434, pp. 9–13, 1991.
- [10] Boffetta G., Ecke R.E., "Two-Dimensional Turbulence". *Annual Review of Fluid Mechanics*, vol. 44 (1), pp. 427–451, 2012.
- [11] Frick P.G., "Turbulence: approaches and models": Institute of Computer Science, pp. 292, (Moscow – Izhevsk), 2003.
- [12] Kraichnan R.H., "Inertial Ranges in Two-Dimensional Turbulence". *Physics of Fluids*, vol. 10(7), pp. 1417-1423, 1967.
- [13] Danilov S.D., Gurarie D., "Quasi-two-dimensional turbulence ". *Physics-Uspexhi*, t. 170, No. 9, pp. 923-928, 2000.
- [14] Bolshukhin M.A., Znamenskaya I.A., Fomichev V.I. "A method of quantitative analysis of rapid thermal processes through vessel walls under nonisothermal liquid flow". *Doklady Physics*, vol. 60, pp. 524–527, 2015.
- [15] Patent RU № 2677793 from 30.09.2014.
- [16] Prah S., «Optical absorption of water» [http://omlc.org.edu/spectra/water/\(2012\)](http://omlc.org.edu/spectra/water/(2012)).
- [17] Warhaft Z., "Passive scalars in turbulent flows". *Annual Reviews of Fluid Mechanics*, vol. 32, pp. 203-240, 2000.